Analyst

PAPER

View Article Online
View Journal | View Issue

Cite this: *Analyst*, 2014, **139**, 1644

Quadruplex priming amplification for the detection of mRNA from surrogate patient samples†

N. M. Adams,[ab] K. K. A. Wang,‡[a] A. C. Caprioli,§[b] L. C. Thomas,¶[a] B. Kankia,[c] F. R. Haselton[b] and D. W. Wright*[a]

Received 9th December 2013
Accepted 27th January 2014

DOI: 10.1039/c3an02261g

www.rsc.org/analyst

Simple and rapid methods for detecting mRNA biomarkers from patient samples are valuable in settings with limited access to laboratory resources. In this report, we describe the development and evaluation of a self-contained assay to extract and quantify mRNA biomarkers from complex samples using a novel nucleic acid-based molecular sensor called quadruplex priming amplification (QPA). QPA is a simple and robust isothermal nucleic acid amplification method that exploits the stability of the G-quadruplex nucleotide structure to drive spontaneous strand melting from a specific DNA template sequence. Quantification of mRNA was enabled by integrating QPA with a magnetic bead-based extraction method using an mRNA–QPA interface reagent. The assay was found to maintain >90% of the maximum signal over a 4 °C range of operational temperatures (64–68 °C). QPA had a dynamic range spanning four orders of magnitude, with a limit of detection of ~20 pM template molecules using a highly controlled heating and optical system and a limit of detection of ~250 pM using a less optimal water bath and plate reader. These results demonstrate that this integrated approach has potential as a simple and effective mRNA biomarker extraction and detection assay for use in limited resource settings.

Introduction

Many methods are used to extract and detect mRNA biomarkers found in patient samples for diagnosing pathogenic infections. These methods often involve multiple steps to perform and commonly require expensive laboratory equipment or trained technicians. For example, reverse transcriptase-polymerase chain reaction (RT-PCR) is commonly used to identify RNA disease biomarkers from patient samples but requires complex and time-consuming sample purification and preparation strategies that are inaccessible to individuals in settings with limited resources because of training, electricity, or financial constraints.[1,2] Simple rapid diagnostic tests based on lateral flow sample processing and antibody binding are commonly used in limited resource settings, but despite being easy to use, they are not effective in many cases for two primary reasons: non-target molecules present in patient samples often interfere with detection, and target biomarkers are often present low abundance.[2–5] Therefore, better methods for purifying and detecting biomarkers of disease in patient samples are needed in settings with limited access to laboratory resources and trained personnel.

The four-stranded G-quadruplex nucleotide structure has been exploited as a platform for a variety of novel nucleic acid detection assays because of its unique stability and folding characteristics. The quadruplex structure is thermodynamically more stable than duplex DNA[6,7] and has been developed to detect short nucleic acid sequences, such microRNAs, that are inaccessible by traditional PCR.[8] In general, these assays are designed to promote the formation of G-quadruplex structures by complementary base pairing with the target nucleic acids and use colorimetric or fluorescence means to monitor the formation of the quadruplex structures. Many groups have taken advantage of the peroxidase-like activity of the G-quadruplex/hemin complex to produce a colorimetric dye in the presence of a target nucleic acid.[8–10] Some of these peroxidase-like amplification assays have been reported to achieve extremely low detection limits,[11,12] yet outside of carefully controlled laboratory conditions, the assays are limited by the highly unstable peroxide reagents and the degradation of the exposed hemin complex.[13] Other groups have monitored the formation of the G-quadruplex structures using quadruplex-specific intercalating dyes[14–16] or Förster resonance energy

[a]*Department of Chemistry, Vanderbilt University, Nashville, Tennessee, 37235, USA. E-mail: david.wright@vanderbilt.edu; Tel: +1-615-322-2636*

[b]*Department of Biomedical Engineering, Vanderbilt University, Nashville, Tennessee, 37235, USA*

[c]*Department of Chemistry and Biochemistry, Ohio State University, Columbus, Ohio, 43210, USA*

† Electronic supplementary information (ESI) available: Supplementary Fig. 1 and Table 1. See DOI: 10.1039/c3an02261g

‡ Present address: Department of Chemistry, University of Illinois at Urbana-Champaign, Urbana, IL 61801, USA.

§ Present address: School of Aeronautics and Astronautics, Purdue University, West Lafayette, Indiana, 47907, USA.

¶ Present address: Department of Life and Physical Sciences, Fisk University, Nashville, Tennessee, 37208, USA.

transfer (FRET) pairs.[17] Some of these methods have been demonstrated to detect nucleic acids in the mid-pM range,[16,17] yet only when performed in simple sample matrices (*i.e.*, buffer) under optimal conditions or over the course of many hours.

Quadruplex priming amplification (QPA) is an isothermal amplification reaction that is also based on the thermodynamic stability of the G-quadruplex structure. QPA has been demonstrated to function as a robust molecular switch, producing fluorescence in the presence of template oligonucleotides with high sensitivity and specificity.[6,18–20] A schematic of the QPA reaction is shown in Fig. 1A. The reaction functions much like polymerase chain reaction, but does not require costly and complex thermal cycling. The reaction begins when a 13-nucleotide QPA primer precursor to the 15-nucleotide G-quadruplex sequence anneals to a complementary template molecule. After annealing, a polymerase enzyme extends the 3′ end of the QPA primer with the guanine nucleotides required to complete the G-quadruplex sequence. Because the stability of the G-quadruplex structure is greater than that of the duplex DNA, thermodynamic factors drive the spontaneous self-dissociation of the duplex.[6] Once the G-quadruplex forms, the template is released and is free to anneal to another primer and start the next cycle of amplification. The G-quadruplex products of the QPA reaction are detected using the incorporated fluorescent nucleotide, 6-methyl isoxanthopterin (6-MI) (depicted in Fig. 1B), a guanosine analog used for studying nucleic acid structures.[21] The 6-MI dye functions as a readout for the QPA assay as it fluoresces intensely when the oligonucleotide is folded into a G-quadruplex structure but is suppressed in the single- and double-stranded states. This occurs because 6-MI fluorescence is quenched when π–π stacked with surrounding nucleotides, whereas in the parallel G-quadruplex structure, 6-MI forms the chain-reversal loop between guanine-quartets and protrudes into the solvent, unquenched by the surrounding nucleotides (Fig. 1C).[19]

Although QPA has been found to be an effective nucleic acid amplification method, the challenge as it relates to biomarker detection is that QPA is limited to the amplification of a single unique template oligonucleotide sequence complementary to the G-quadruplex sequence and not biomarker target sequences. In these studies, we develop an mRNA–QPA interface reagent, which contains the 15-nucleotide template sequence linked to a 22-nucleotide probing sequence complementary to the mRNA biomarker. This interface reagent enables indirect QPA detection of mRNA biomarkers by associating mRNA biomarker targets with the templates.

The implementation of the interface reagent is facilitated using our previously described self-contained extraction format.[3–5,22] This self-contained format for biomarker extraction has been used to process RNA, DNA, and protein biomarkers from complex samples to improve RT-PCR, PCR, and lateral flow detection, respectively.[3–5] In this format, sample processing is carried out in small diameter tubing by pulling functional magnetic beads bound to target biomarkers through processing solutions that are separated by surface tension valves. Surface tension valves (*i.e.*, air or oil separators) keep the solutions within the tubing stationary while permitting the transport of magnetic beads across the interface.[22] The advantages of the self-contained format are that it facilitates complex sample processing steps with the use of simple magnetic bead manipulation using a permanent magnet, enables the assay to be performed without the use of pipettes or other laboratory equipment, and protects the assay contents from environmental contaminants.

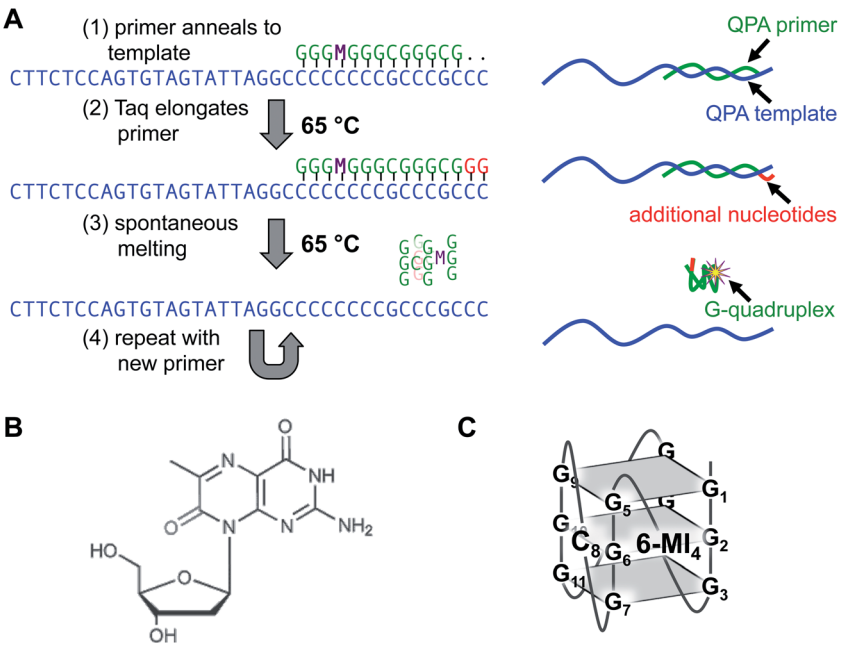

Fig. 1 (A) Schematic of the isothermal quadruplex priming amplification (QPA) method. The guanosine analog 6-methyl isoxanthopterin (6-MI) is denoted with the letter M. The QPA template sequence (blue) is abbreviated for simplicity. (B) Chemical structure of the 6-MI dye used in QPA. (C) Illustration of the parallel G-quadruplex product of QPA.

We have integrated this self-contained format to enable the detection of mRNA from surrogate patient sample matrices by QPA. The complete assay functions by extracting mRNA biomarkers from a complex sample on the surface of a magnetic bead, binding the magnetic bead-captured mRNA biomarkers with QPA template sequences using an mRNA–QPA interface reagent, and delivering the bead/mRNA/interface reagent complex into a final QPA reaction solution for detection (Fig. 2). The interface reagent determines specificity of the assay; if the specific mRNA biomarkers are present, the interface reagents are delivered to the QPA reaction for amplification. In this report, we describe the development and evaluation of the three critical components that make this integrated assay possible: (i) self-contained extraction of mRNA using magnetic beads, (ii) conversion of mRNA biomarkers to QPA templates using the mRNA–QPA interface reagent, and (iii) optimization of the sensitivity and dynamic range of QPA.

Results and discussion

6-Methyl isoxanthopterin-labeled G-quadruplex as a molecular sensor

Our first objective was to establish the 6-MI-labeled G-quadruplex sequence as an effective molecular sensor under the conditions of our assay. QPA signal depends on a significant difference in fluorescence intensity between the single-stranded state of the 6-MI-labeled QPA primer (G4BK_primer_6MI@4) and the G-quadruplex product (G4BK_+primer_6MI@4). We compared the relative fluorescence intensity of increasing concentrations of the two oligonucleotides. The results show that the G-quadruplex product had a ~25-fold fluorescence enhancement over the QPA primer, which established it as an effective molecular sensor (Fig. 3A).

To validate that this fluorescence enhancement correlated with a G-quadruplex structure, circular dichroism was performed on the oligonucleotide samples. The single-stranded mRNA–QPA interface reagent oligonucleotide was also analyzed as a control. The circular dichroism spectrum of the G-quadruplex product had a minimum at 241 nm, strong maxima at 210 and 262 nm, and a slight maximum at 300 nm (Fig. 3B). These results are characteristic of a parallel quadruplex nucleotide structure.[19,23] The single-stranded QPA primer, on the other hand, had a spectrum consistent with oligonucleotides with high GC content, with a maximum at 264 nm and a minimum at 238 nm. The single-stranded interface reagent had a spectrum with a maximum at 276 and a minimum at 243 nm, characteristic of single-stranded oligonucleotides.

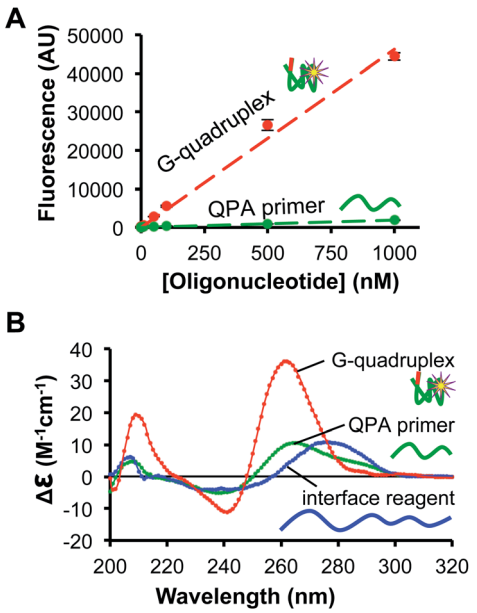

Fig. 3 The 6-MI-labeled G-quadruplex is an effective molecular sensor. (A) 6-MI has a ~25-fold fluorescence enhancement in the G-quadruplex product compared to the single-stranded QPA primer (mean ± σ, n = 3). (B) Circular dichroism (CD) spectra of the components of the QPA reaction. The CD spectrum of the elongated QPA primer (red) is consistent with a parallel G-quadruplex structure, while the spectra of the QPA primer precursor (green) is consistent with single-stranded DNA.

Together, these data indicate that 6-MI is effectively quenched in the single-stranded state and that the fluorescence is enhanced ~25-fold when the two nucleotides are added to complete the sequence necessary to form the G-quadruplex. This signal-to-noise ratio under these ideal conditions is exceptional compared to the 3- to 10-fold ratios reported for other G-quadruplex-based amplification assays.[8,11,14–17] These results validate 6-MI-labeled G-quadruplex as a potential molecular sensor.

Optimizing and evaluating QPA for sensitivity

The next step was to optimize and evaluate the sensitivity and dynamic range of QPA (integration component (iii) from Fig. 2). Because QPA is a linear amplification method, the most

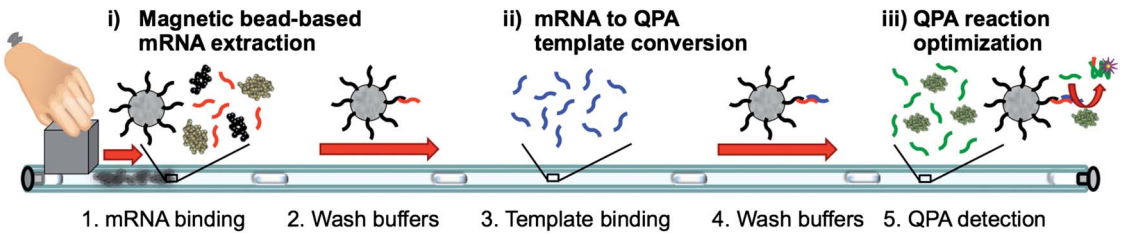

Fig. 2 Schematic representation of the integrated self-contained mRNA extraction and QPA amplification assay. The three critical components for integration (i–iii) and the assay processing steps (1–5) are identified.

effective measure of efficiency is the slope of the response curve (*i.e.*, the change in fluorescence signal per unit time). In these studies, a variety of conditions were tested using Qiagen's Rotor-Gene Q real-time PCR instrument to monitor the change in fluorescence in real-time. The optimal temperature was determined by running the QPA reaction at six different temperatures from 61 °C to 71 °C using a set of baseline reaction conditions (QPA buffer, 2.5 μM QPA primer, 0.05 units per μL polymerase, 0.5 mM dGTP, 0% trehalose, 1 nM mRNA–QPA interface reagent). While the optimal reaction temperature was determined to be 65–66 °C, QPA was found to maintain >90% of the maximum signal from approximately 64 to 68 °C (Fig. 4A). Using the baseline reaction conditions and a 65 °C reaction temperature, a range of primer concentrations from 0 to 10 μM were then tested. Optimal signal was produced using a 5 μM primer concentration (Fig. 4B). At 5 μM concentration, however, the background signal from the QPA primers disproportionately increased, which decreased the signal-to-noise ratio and the dynamic range. Therefore, a 2.5 μM primer concentration was determined as optimal. Next, a range of polymerase concentrations from 0 to 0.5 units per μL was tested. Polymerase concentration had a significant impact on the signal produced, resulting in a signal ~3-fold greater at 0.25 units per μL compared to the 0.05 units per μL baseline concentration (Fig. 4C). Because of the cost of the commercial polymerase, 0.15 units per μL was determined to be the most economical concentration as it falls within ~20% of the optimal signal yet uses 40% less enzyme. The effect of adding trehalose sugar was also evaluated. Trehalose sugar has historically been used to stabilize enzymatic reagents for lyophilization and long-term storage.[24,25] One group also reported that the addition of trehalose sugar to polymerase chain reaction increases the efficiency of amplification of GC-rich templates by reducing the DNA melt temperature and thermally stabilizing the polymerase enzyme.[26] Consistent with these findings, the signal generated from the QPA reaction, which amplifies templates that are composed exclusively of GC nucleotides, increased linearly from 0% to 10% trehalose, effectively doubling the signal of the reaction (Fig. 4D). Concentrations greater than 10% trehalose had less effect on signal; therefore, a 10% trehalose concentration was determined to be optimal. Overall, a 3- to 4-fold increase in signal was achieved over the course of these optimization studies.

Using the optimized reaction conditions, the limit of detection and dynamic range of the QPA reaction was determined. A series of mRNA–QPA interface reagent concentrations were added to the QPA reaction, and the Rotor-Gene Q instrument monitored the change in fluorescence over a period of 45 minutes at 65 °C. The data that was collected produced a series of linear response curves with slopes proportional to the concentration of interface reagents present in the reaction (Fig. 5A). The slopes of these response curves were plotted against their respective interface reagent concentrations to generate a standard curve for quantification (Fig. 5B). Based on these data obtained under optimal conditions, the limit of detection was determined to be 24 pM mRNA–QPA interface reagents. Using a greater range of interface reagent concentrations, it was determined that the dynamic range spans nearly 4 orders of magnitude (~20 pM to ~100 nM) (ESI Fig. 1†). These data demonstrate that the QPA reaction effectively quantifies interface reagents at low sensitivity and across a relatively wide range of concentrations.

mRNA–QPA interface reagent enables mRNA detection by QPA

To be useful as a readout for a diagnostic test, QPA templates must be associated with an mRNA biomarker characteristic of a particular disease. We developed an mRNA–QPA interface reagent for associating mRNA biomarkers with QPA templates

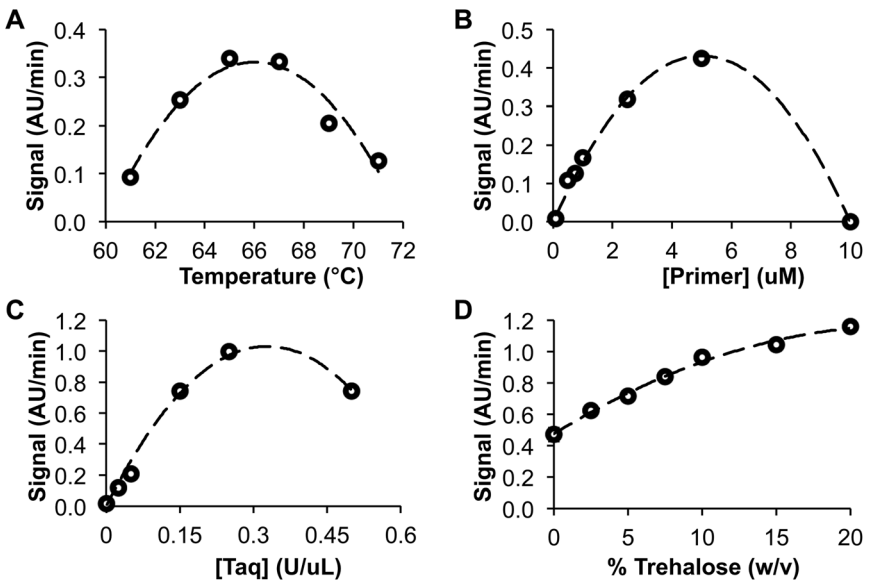

Fig. 4 The optimal QPA signal was determined by testing a range of temperatures (A), QPA primer concentrations (B), Taq polymerase concentrations (C), and trehalose concentrations (D) (mean ± σ, $n = 3$).

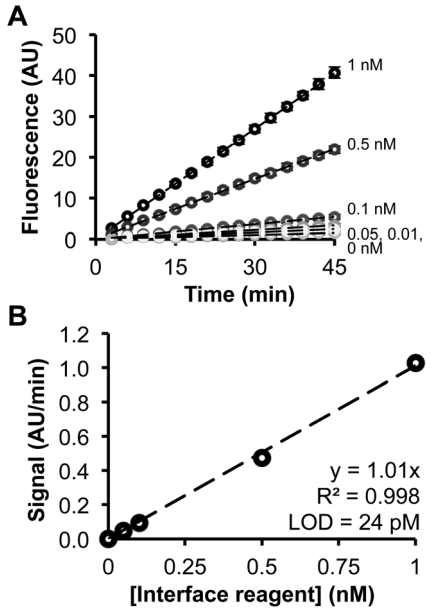

Fig. 5 Isothermal QPA is a linear and quantitative amplification method as measured in real-time using a Rotor-Gene Q PCR instrument. (A) QPA signal results in linear increase of fluorescence for each interface reagent concentration during the course of the reaction (mean ± σ, $n = 3$). (B) The increase in fluorescence during the QPA reaction is directly proportional to the concentration of interface reagents present in the reaction. Based on these data, a limit of detection of 24 pM interface reagents was calculated by multiplying three times the standard deviation of the QPA signal from each interface reagent concentration and using the slope of the linear range of the standard curve to derive the value (mean ± σ, $n = 3$).

to enable QPA detection of these mRNA targets (research focus (ii) from Fig. 2). This mRNA–QPA interface reagent is key for introducing sequence specificity in the presence of bulk mRNA on the surface of the oligo-dT functionalized beads; only if the specific mRNA biomarker is present will the template sequence of the mRNA–QPA interface reagent be delivered to the QPA reaction. The interface reagent contains a 22-nucleotide probing region complementary to an mRNA biomarker, a 5-nucleotide spacer, and the 15-nucleotide template sequence for QPA. The complete integrated assay involves isolating mRNA biomarkers from complex samples using oligo-dT functionalized magnetic particles, and then probing for the mRNA biomarkers with the mRNA–QPA interface reagent. The QPA reaction is then used to indirectly quantify the mRNA by amplifying from the template portion of the mRNA–QPA interface reagent. A schematic representation of the physical layout of the assay is depicted in Fig. 2. Each step of the assay takes place inside of 1.6 mm ID Tygon tubing by simply pulling the magnetic particles through processing solutions separated by surface tension valves, until the last step, where QPA spontaneously initiates amplification upon the delivery of the interface reagents.

To determine the efficiency of the mRNA extraction assay in the presence of background biomolecules (integration component (i) from Fig. 2), mRNA biomarkers were extracted from solutions containing Tris–HCl buffer (pH 8.0), ~2.5 ng μL^{-1} non-target yeast total RNA (~100-fold more RNA than the mRNA biomarker), or a surrogate nasal wash sample containing HEp-2 cell lysate. Each of the samples was spiked with 30 pmol mRNA biomarker. Although virtually any mRNA sequence could be used as a demonstration of feasibility, the sequence used in these studies is based on a 38 nucleotide sequence from the respiratory syncytial virus nucleocapsid gene mRNA to which a 22-nucleotide poly-A tail was added. Extraction of the mRNA was then carried out by pulling the beads through the wash buffers and into a Tris–HCl buffer (pH 8.0) elution solution. The concentration of the labeled mRNA biomarkers in the final solution was determined using fluorescence spectroscopy. Extraction yields from the sample matrices was ~35% of the starting amount of mRNA biomarker, and there was no statistical difference among the three sample types (Fig. 6A). Notably, the biomarkers are concentrated 2.5-fold through the extraction process (the initial binding solution is 250 μL and the final elution solution is 100 μL); therefore, the effective biomarker enrichment is nearly 90% of the starting concentration. These results indicate that the mRNA extraction method is robust and compatible with sample matrices of increasing complexity.

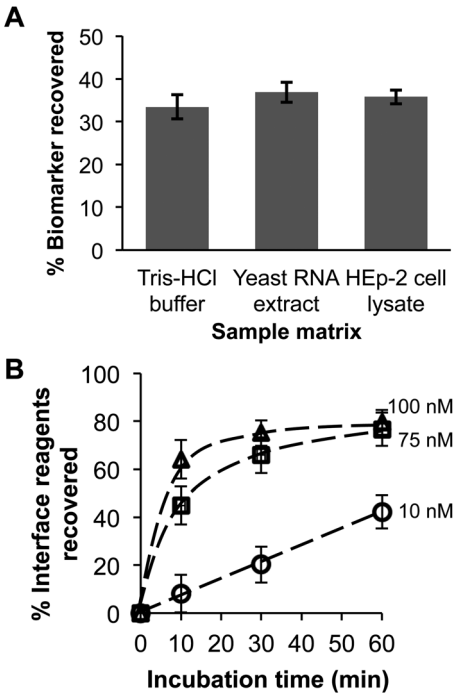

Fig. 6 The self-contained format is effective for extracting mRNA biomarkers from complex samples and associating biomarkers with mRNA–QPA interface reagents. (A) Extraction of the synthetic mRNA biomarker sequence is effective in the self-contained format using oligo dT-functionalized magnetic beads. mRNA was extracted from solutions of increasing complexity: Tris–HCl buffer at pH 8.0, yeast RNA extract at 100-fold the amount of target mRNA, or Hep-2 cell lysate at 10^5 cells per mL (mean ± σ, $n = 3$). (B) The number of interface reagents recovered (*i.e.*, the number of interface reagents associated with mRNA biomarkers) increases with incubation time and interface reagent concentration in the template binding solution (circles = 10 nM, squares = 75 nM, and triangles = 100 nM) (mean ± σ, $n = 3$).

The efficiency of mRNA–QPA interface reagent binding to mRNA biomarker was evaluated next (integration component (ii) from Fig. 2) by testing 10 to 100 nM interface reagent concentrations and 10 to 60 minute incubation times in the template binding solution. The amount of interface reagents eluted into Tris–HCl buffer was measured using fluorescence spectroscopy and expressed relative to the amount of biomarker recovered in the same solution. The data show that the amount of interface reagent recovered increased with template concentration and with incubation time, resulting in a maximum interface reagent yield of nearly 80% of the amount of recovered mRNA biomarkers using a 100 nM interface reagent concentration and a 60 minute incubation time (Fig. 6B). An interface reagent concentration of 75 nM was chosen, however, to limit the amount of interface reagent that would be nonspecifically pulled through with solution carry-over, and an incubation time of 30 minutes was chosen to decrease the overall assay time. Under these conditions, the mRNA–QPA interface reagent yield was 66% of the amount of the recovered mRNA biomarkers.

These data demonstrate that this self-contained assay based on oligo-dT functionalized magnetic beads and surface tension valves effectively associates mRNA–QPA interface reagents with mRNA biomarkers preparatory to running isothermal QPA. The overall effective delivery of interface reagents to the final solution is ~60%, relative to the concentration of mRNA biomarkers present in the initial binding solution. Although this effective yield is sufficient for a demonstration of feasibility, there may be instances where it may need to be increased. As demonstrated in previous biomarker extraction and concentration studies[5], by simply decreasing the elution solution volume, the final interface reagent concentration can be increased.

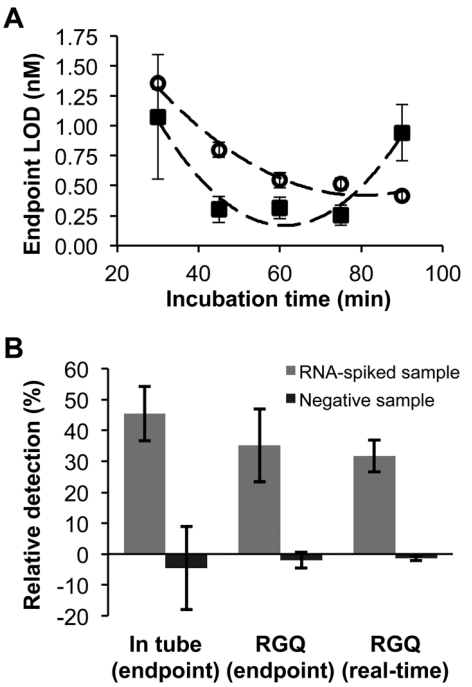

Fig. 7 Isothermal QPA performs well when heated within the self-contained format in a water bath. (A) The limits of detection based on endpoint fluorescence measurements at a range of incubation time points of the in-tube QPA reaction heated by water bath (solid squares) compared to QPA reaction heated in the Rotor-Gene Q (open circles) (mean $\pm \sigma$, $n = 3$). (B) Detection of the synthetic mRNA biomarker from RNA-spiked (gray bars) and unspiked (black bars) surrogate nasal wash samples after self-contained extraction and QPA template binding. Three QPA reaction conditions are compared after a 45 minute incubation: (i) water bath heated within a tube, endpoint measured (left bars); (ii) Rotor-Gene Q heated, endpoint measured (middle bars); and (iii) Rotor-Gene Q heated, measured in real-time (right bars). QPA signal is expressed as a percentage of the total possible signal given a starting mRNA concentration of 1.2 nM (mean $\pm \sigma$, $n = 3$).

Self-contained mRNA extraction and detection

To determine the efficacy of QPA within the self-contained tube format, QPA performance was evaluated at 30, 45, 60, 75, and 90 minute time points after incubating the tubes at 65 °C in a circulating water bath. In this format, real-time monitoring of the QPA reaction was not feasible, so endpoint fluorescence measurements were collected after the tubes were pulled from the water bath. The data show that limits of detection between ~300 and ~250 pM mRNA–QPA interface reagents were achieved when incubated in the tube for 45, 60, and 75 minutes (Fig. 7A, solid squares). At the 30 and 90 minute time points, the limits of detection of the in-tube QPA assay were worse, at ~1 nM. These data demonstrate that 30 minutes is not long enough to get consistent signal and that at 90 minutes signal begins to plateau. A 45 minute incubation time was used for subsequent assays, as it was the earliest time point that resulted in a reasonable limit of detection (300 nM). These limits of detection are over one order of magnitude worse than the QPA reaction monitored in real-time using the Rotor-Gene Q PCR instrument (see Fig. 5B). To determine if this was an effect of the less precise heating method or the endpoint measurement method, endpoint measurements of the QPA reaction were also collected using the Rotor-Gene Q instrument. Under the precise thermal control of the Rotor-Gene Q instrument, the limit of detection at 30 minutes was 1.4 nM mRNA–QPA interface reagents and decreased steadily with increasing incubation times, approaching a lower limit of ~400 pM mRNA–QPA interface reagents at 90 minutes (Fig. 7A, open circles). These data demonstrate that the QPA reaction performs well while being heated in a water bath within the self-contained format, achieving limits of detection on par with the more precise, thermally controlled Rotor-Gene Q instrument. Because of these observations, we hypothesize that real-time monitoring of the in-tube QPA reaction will achieve the limits of detection of the real-time Rotor-Gene Q instrument. Current efforts are focused on developing an instrument format for heating and reading fluorescence of the QPA reaction performed within the self-contained format.

The performance of the integrated self-contained mRNA extraction and QPA detection assay was evaluated next. The assay was performed using surrogate patient samples positive for the synthetic mRNA biomarker (30 pmol mRNA spiked into HEp-2 lysates) and negative for the mRNA biomarker (unspiked). After loading the sample containing the magnetic

beads, the entire assay was performed within the assay tube, including mRNA extraction, mRNA–QPA interface reagent binding, and QPA amplification. The QPA reaction solution was removed after a 45 minute incubation time and the contents were endpoint detected using a benchtop plate reader. This method resulted in the detection of ~45 ± 8.9% of mRNA–QPA interface reagents relative to the mRNA content in the RNA-spiked sample and −4.5 ± 13% in the negative sample (Fig. 7B, left gray bar and left black bar, respectively). For comparison, the same samples were tested using the Rotor-Gene Q instrument for the QPA incubation and detection step, while the mRNA extraction and template binding steps remained in the self-contained format. The results from the Rotor-Gene Q instrument was comparable to the in-tube method, detecting 35 ± 12% mRNA–QPA interface reagents relative to the mRNA content in the RNA-spiked sample and −2.0 ± 2.5% in the negative sample when measured at the 45 minute endpoint. Using real-time monitoring of QPA outside of the tubing, the quantification of the mRNA–QPA interface reagent was 32 ± 5.1% relative to the mRNA content in the RNA-spiked sample and −1.5 ± 0.7% in the negative samples (Fig. 7B). These data show that monitoring the QPA reaction in real-time produces much more consistent results, while endpoint measurements of QPA result in a substantial amount of error.

These data demonstrate that isothermal QPA performs well when heated in a simple water bath and detected using a plate reader, achieving a limit of detection of ~250 pM mRNA–QPA interface reagents bound to mRNA. We found the complete self-contained mRNA extraction and QPA detection assay to be specific, detecting between ~35 and ~45% of the potential interface reagents relative to the initial concentration of synthetic mRNA biomarkers in the biomarker-spiked surrogate nasal wash samples, while detecting virtually no signal in the negative control samples, despite containing a high background of non-target mRNA molecules from the HEp-2 cell lysates. Based on a 45% relative detection of mRNA biomarkers, the effective limit of detection of the complete integrated assay is ~560 pM mRNA biomarkers from a surrogate patient sample. These data also reveal that real-time monitoring of the change in fluorescence over the course of the reaction (*i.e.*, the slope fluorescence response curve) produces more consistent results than endpoint analysis of the samples (compare the error in Fig. 5B to Fig. 7A). This is likely because variation in the baseline or starting fluorescence of individual samples does not affect the slope of the fluorescence response curve, yet influences values of the endpoint analysis. Therefore, methods to monitor real-time fluorescence of the QPA reaction are necessary to achieve the optimal sensitivity and specificity in the self-contained mRNA extraction and QPA detection assay.

Experimental

Oligonucleotide synthesis

The oligonucleotides used in these studies include QPA primers, mRNA–QPA interface reagents, and a synthetic mRNA biomarker (ESI Table 1†). The QPA primer oligonucleotides containing the 6-MI dye were synthesized at a 200 nmole scale by Fidelity Systems, Inc. and purified by desalting. The mRNA–QPA interface reagents and the synthetic mRNA biomarker oligonucleotide were synthesized by Integrated DNA Technologies at 250 nmole scale and purified using high performance liquid chromatography. Although virtually any mRNA sequence could be used as a demonstration of feasibility, the sequence used in these studies is based on a 38 nucleotide sequence from the respiratory syncytial virus nucleocapsid gene mRNA. The synthetic 22-nucleotide adenine tail was added to this sequence to enable extraction using oligo-dT beads. Upon arrival, the oligonucleotides were resuspended to a concentration of ~100 mM in molecular grade water (cat. no. BP2819-4, Fisher Scientific) and stored at −20 °C until use.

Circular dichroism of QPA oligonucleotides

An Aviv circular dichroism (CD) spectrometer (mod. no. 215, Aviv Biomedical, Inc.) was used to collect CD spectra of the single-stranded and quadruplex DNA molecules. Oligonucleotides were prepared at a 100 μM base concentration in QPA buffer (10 mM Tris HCl, pH 8.7, 2 mM $MgCl_2$, 25 mM KCl, 25 mM CsCl). Each sample was heated in 1 mL tubes to 90 °C for 5 minutes and cooled slowly over the course of 1 hour to room temperature by controlling the heat block temperature. The samples were analyzed using a 1 cm path length CD cell. The spectra were collected at 25 °C from 320 nm to 200 nm using a 1 nm step, a 1.0 nm bandwidth, and a 2 second averaging time. At least three spectra from each sample collected, averaged, and smoothed using the using CD-215 software version 2.90 provided by the manufacturer. The spectra were normalized by subtracting the CD spectrum generated from a blank sample (QPA buffer only) collected under the same conditions.

6-Methyl isoxanthopterin (6-MI) fluorescence measurements

Solutions of QPA primer or G-quadruplex oligonucleotides were prepared in triplicate at 10, 50, 100, 500, and 1000 nM concentrations. Each solution was heated to 90 °C for 5 min and cooled over the course of 1 hour to room temperature. One hundred microliters of each solution was added to a well of a black Costar round bottom 96-well plate. Fluorescence measurements were collected in triplicate using a BioTek Synergy H4 Hybrid 96-well plate reader using an excitation wavelength of 340 nm and a detection wavelength of 430 nm.

Optimizing the quadruplex priming amplification reaction

Unless otherwise noted, QPA reactions were carried out in a 100 μL volume containing QPA buffer (10 mM Tris HCl, pH 8.7, 2 mM MgCl2, 25 mM KCl, 25 mM CsCl), 2.5 μM QPA primer (G4BK_primer_6MI@4), 0.15 units per μL AmpliTaq DNA Polymerase (cat. no. P15533, Roche), 0.5 mM dGTP (cat. no. R0161, Thermo Scientific), and 10% w/v Trehalose (cat. no. 90210-50G, Sigma Aldrich). Each reaction solution was split into three thin-walled PCR tubes (cat. no. 981005, Qiagen), with 25 μL in each tube. The reaction ran at 65 °C in the Rotor-Gene Q 6-plex thermal cycler (cat. no. 9001720, Qiagen) and real-time fluorescence measurements were collected every three minutes using an excitation wavelength of 365 nm and a detection

wavelength of 460 nm for detecting the 6-methyl isoxanthopterin dye in the G-quadruplex product. QPA reactions with 0, 0.05, 0.1, 0.5, and 1 nM mRNA–QPA interface reagent (QPA template) concentrations were run in triplicate and in parallel and were used as a standard curve. The lower limit of detection was calculated using the following formula: $LOD = 3\sigma + m$, where σ is the average of three standard deviation measurements of the QPA signal from each interface reagent concentration and m is the slope as calculated by the best-fit trendline of the linear range of the standard curve.

Preparation of the self-contained processor

Prior to processing a sample, the solutions of the self-contained processor were preloaded by serially injecting the solutions in reverse order through one end of 1.6 mm ID Tygon R-3603 tubing (Saint-Gobain). Unless otherwise noted, the processing solutions and volumes used in the self-contained processor where adapted from the Life Technologies Dynabeads Oligo (dT)25 (cat. no. 61005) product manual. The final processing solution was loaded into the tubing first by injecting 100 μL of 10 mM Tris–HCl buffer (pH 8.0) for studies to determine biomarker and mRNA–QPA interface reagent yield or 100 μL of QPA reaction solution for studies on QPA detection. To separate this solution from the next one, a surface tension valve, or air bubble spacer, was formed by slightly tilting the tubing until the solution moved ~1 cm away from the end of the tubing. This procedure was followed after injecting each of the following solutions. Three post-template wash solutions were then loaded by injecting 100 μL of wash buffer B (10 mM Tris–HCl, pH 8.0, 150 mM LiCl, 1 mM EDTA) into the tube three times. One hundred microliters of template binding solution was then added by injecting 100 μL of wash buffer B containing 75 nM mRNA–QPA interface reagent (G4BK_temp_RSV22+5 w/Cy5), unless otherwise noted. Another series of wash chambers were then added: 250 μL of wash buffer B, and two solutions of wash buffer A (10 mM Tris–HCl, pH 8.0, 150 mM LiCl, 1 mM EDTA, 0.1% LiDS). The end of the tubing opposite of the loading end was then sealed using a small plug. At this point the preloaded processor was ready for sample loading and processing.

Procedure for self-contained processing of mRNA

The procedure for processing the sample included preparing and injecting the binding solution into the processor tubing followed by pulling the magnetic beads through the processing solutions. The binding solution was prepared with 1 mg Dynabeads Oligo (dT)25 (cat. no. 61005, Life Technologies) resuspended in 225 μL binding/lysis buffer (100 mM Tris–HCl, pH 8.0, 500 mM LiCl, 10 mM EDTA, 1% LiDS). The sample matrices that were used include 100 mM Tris–HCl (pH 8.0), ~2.5 ng μL^{-1} yeast total RNA extract (cat. no. AM7118, Life Technologies), or HEp-2 cell lysate containing 10^5 cells per mL (preparation of this matrix is described in ref. 4), each spiked with 30 pmol synthetic mRNA (RSVN_939-978_mRNA w/HEX). For each sample, 25 μL of the matrix was added to the binding solution and mixed for 10 minutes on a laboratory rotator. The plug was then removed from the processor tubing, the 250 μL binding solution was added to tubing, and the plug was replaced. The magnetic beads were then gathered within the binding solution using a 2.54 cm neodymium cube magnet (SKU no. M1CU, Apex Magnets). The beads were then carefully pulled through the air separator and into the first wash solution. The beads were dispersed within the wash solution for ~5 seconds, gathered, and then pulled into the subsequent solution. These steps were repeated for each of the wash buffer solutions. Once the beads were pulled into the template binding chamber, they were dispersed throughout the chamber, and the processing tube was placed in the dark for 30 minutes, unless otherwise noted. Afterwards, the beads were pulled through the three 100 μL wash buffer B chambers as described above. Finally, the beads were pulled into the final solution for oligonucleotide content analysis or for quantitation by QPA.

For content analysis, the elution solution containing the beads was placed on a heating block for 10 minutes at 85 °C, the supernatant was removed from the beads, and the 40 μL of the supernatant was added to a well of a black Costar round bottom 96-well plate. Fluorescence measurements were collected in triplicate using a BioTek Synergy H4 Hybrid 96-well plate reader with an excitation wavelength of 535 nm and a detection wavelength of 565 nm for the mRNA biomarker (RSVN_939-978 mRNA w/HEX) and with an excitation wavelength of 646 nm and a detection wavelength of 670 nm for the mRNA–QPA interface reagent (G4BK_temp_RSV22+5 w/Cy5), and measurements were compared to standard curves. For quantitation by QPA, the Tygon tube was placed in a water bath for 5 minutes at 85 °C and 45 minutes at 65 °C and endpoint fluorescence measurements were collected in triplicate using an excitation wavelength of 365 nm and a detection wavelength of 460 nm for detecting the 6-methyl isoxanthopterin dye in the G-quadruplex product. QPA reactions with 0, 0.05, 0.1, 0.5, and 1 nM mRNA–QPA interface reagent concentrations were run in parallel and used as a standard curve.

The overall effective delivery yield of mRNA–QPA interface reagents in the final solution was calculated as a percentage relative to the concentration of spiked mRNA biomarkers present in the initial binding solution, and is based on the standard curve of interface reagents. This measurement reflects the efficiency of mRNA extraction and subsequent binding of the interface reagent.

Conclusions

In this report, we described the integration of self-contained mRNA biomarker extraction and isothermal detection based on QPA. The simple assay effectively isolates mRNA biomarkers from complex samples, binds the mRNA biomarkers with mRNA–QPA interface reagents, and deposits them into a final solution for isothermal QPA detection. These results indicate that this system has a number of advantages for use as an mRNA biomarker detection assay. First, the assay is able to detect relatively short RNA molecules, which is not possible using traditional PCR. The biomarker target we tested is 60 nucleotides long; however, it is theoretically reasonably that targets as short as 35 nucleotides could be detected using this

assay while still maintaining reasonable specificity (*i.e.*, 15 nucleotides complementary to the capture sequence on the bead with 15 nucleotides complementary to the mRNA–QPA interface reagent, plus 5 nucleotides in between to prevent steric constraints). Second, the QPA assay is simple and robust. The molecular mechanism does not require a complex series of interactions and events to function, but is carried out at a single temperature with a single primer and polymerase enzyme. Also, the reaction is tolerant of ±2 °C change in operational temperature while maintaining reaction efficiency within 90% of the optimal efficiency. Another advantage of the QPA assay is that it is quantitative over four orders of magnitude and has a lower limit of detection of ~250 pM using an endpoint analysis or ~20 pM using real-time analysis. Furthermore, the complete mRNA extraction and detection assay is self-contained and requires relatively few steps for the end user to complete. The tubing can be preloaded with the assay reagents, so that performing the assay simply consists of injecting the patient sample into the tube, pulling the magnetic beads through the assay solutions, incubating the tube in a water bath, and reading the fluorescence against a standard curve. The total time duration from sample-in to answer-out is ~90 minutes. This approach represents a simple platform that could be applied to other classes of molecular sensors to enable detection of a variety of biomolecular targets from complex samples.

Acknowledgements

This work was supported by the Bill & Melinda Gates Foundation through the Grand Challenges in Global Health initiative to F.R.H. and D.W.W. and to B.K. Support from the National Science Foundation Graduate Research Fellowship Program is gratefully acknowledged by N.M.A. [DGE 0909667]. L.T. acknowledges support from the National Science Foundation REU in Chemical Biology at Vanderbilt University [NSF CHE-1156922]. We are grateful to Adam Taylor, David Gvarjaladze, and Levan Lomidze from The Ohio State University for preliminary experiments and useful discussion.

References

1 A. Niemz, T. M. Ferguson and D. S. Boyle, *Trends Biotechnol.*, 2011, **29**, 240–250.
2 P. Yager, G. J. Domingo and J. Gerdes, *Annu. Rev. Biomed. Eng.*, 2008, **10**, 38.
3 K. M. Davis, J. D. Swartz, F. R. Haselton and D. W. Wright, *Anal. Chem.*, 2012, **84**, 6136–6142.
4 H. Bordelon, N. M. Adams, A. S. Klemm, P. K. Russ, J. V. Williams, H. K. Talbot, D. W. Wright and F. R. Haselton, *ACS Appl. Mater. Interfaces*, 2011, **3**, 2161–2168.
5 H. Bordelon, P. K. Russ, D. W. Wright and F. R. Haselton, *PLoS One*, 2013, **8**, e68369.
6 B. I. Kankia, *Anal. Biochem.*, 2011, **409**, 59–65.
7 P. A. Rachwal, T. Brown and K. R. Fox, *Biochemistry*, 2007, **46**, 3036–3044.
8 S. Nakayama and H. O. Sintim, *J. Am. Chem. Soc.*, 2009, **131**, 10320–10333.
9 Y. Xiao, V. Pavlov, T. Niazov, A. Dishon, M. Kotler and I. Willner, *J. Am. Chem. Soc.*, 2004, **126**, 7430–7431.
10 D. M. Kolpashchikov, *J. Am. Chem. Soc.*, 2008, **130**, 2934–2935.
11 S. Shimron, F. Wang, R. Orbach and I. Willner, *Anal. Chem.*, 2011, **84**, 1042–1048.
12 F. Wang, L. Freage, R. Orbach and I. Willner, *Anal. Chem.*, 2013, **85**, 8196–8203.
13 X. Yang, C. Fang, H. Mei, T. Chang, Z. Cao and D. Shangguan, *Chem. – Eur. J.*, 2011, **17**, 14475–14484.
14 Y. Guo, P. Xu, H. Hu, X. Zhou and J. Hu, *Talanta*, 2013, **114**, 138–142.
15 J. Ren, J. Wang, J. Wang, N. W. Luedtke and E. Wang, *Biosens. Bioelectron.*, 2012, **31**, 316–322.
16 C. Zhao, L. Wu, J. Ren and X. Qu, *Chem. Commun.*, 2011, **47**, 5461–5463.
17 Q. Yue, T. Shen, C. Wang, L. Wang, H. Li, S. Xu, H. Wang and J. Liu, *Biosens. Bioelectron.*, 2012, **40**, 75–81.
18 A. Taylor, A. Joseph, R. Okyere, S. Gogichaishvili, K. Musier-Forsyth and B. Kankia, *Biophys. Chem.*, 2012, **171**, 1–8.
19 J. Johnson, R. Okyere, A. Joseph, K. Musier-Forsyth and B. Kankia, *Nucleic Acids Res.*, 2013, **41**, 220–228.
20 S. Gogichaishvili, J. Johnson, D. Gvarjaladze, L. Lomidze and B. Kankia, *Biopolymers*, 2013, DOI: 10.1002/bip.22421.
21 K. Datta, N. P. Johnson, G. Villani, A. H. Marcus and P. H. von Hippel, *Nucleic Acids Res.*, 2012, **40**, 1191–1202.
22 N. M. Adams, A. E. Creecy, C. E. Majors, B. A. Wariso, P. A. Short, D. W. Wright and F. R. Haselton, *Biomicrofluidics*, 2013, **7**, 014104.
23 J. Kypr, I. Kejnovska, D. Renciuk and M. Vorlickova, *Nucleic Acids Res.*, 2009, **37**, 1713–1725.
24 J. Tomlinson, N. Boonham, K. Hughes, R. Griffin and I. Barker, *Appl. Environ. Microbiol.*, 2005, **71**, 6702–6710.
25 P. R. Klatser, S. Kuijper, C. W. van Ingen and A. H. Kolk, *J. Clin. Microbiol.*, 1998, **36**, 1798–1800.
26 A.-N. Spiess, N. Mueller and R. Ivell, *Clin. Chem.*, 2004, **50**, 1256–1259.

